PHYSICAL REVIEW FLUIDS **2**, 052301(R) (2017)

Segregation physics of a macroscale granular ratchet

Ashish Bhateja* and Ishan Sharma†
Mechanics & Applied Mathematics Group, Department of Mechanical Engineering, Indian Institute of Technology Kanpur 208016, Uttar Pradesh, India

Jayant K. Singh‡
Department of Chemical Engineering, Indian Institute of Technology Kanpur 208016, Uttar Pradesh, India
(Received 27 June 2016; revised manuscript received 22 March 2017; published 10 May 2017)

New experiments with multigrain mixtures in a laterally shaken, horizontal channel show complete axial segregation of species. The channel consists of multiple concatenated trapeziums, and superficially resembles microratchets wherein asymmetric geometries and potentials transport, and sort, randomly agitated microscopic particles. However, the physics of our macroscale granular ratchet is fundamentally different, as macroscopic segregation is gravity driven. Our observations are not explained by classical granular segregation theories either. Motivated by the experiments, extensive parallelized discrete element simulations reveal that the macroratchet differentiates grains through hierarchical bidirectional segregation over two different time scales: Grains rapidly sort vertically into horizontal bands spanning the channel's length that, subsequently, slowly separate axially, driven by strikingly gentle, average interfacial pressure gradients acting over long distances. At its maximum, the pressure gradient responsible for axial separation was due to a change in height of about two big grain diameters ($d = 7$ mm) over a meter-long channel. The strong directional segregation achieved by the granular macroratchet has practical importance, while identifying the underlying new physics will further our understanding of granular segregation in industrial and geophysical processes.

DOI: 10.1103/PhysRevFluids.2.052301

I. INTRODUCTION

Microscopic many-particle systems, such as molecules or biopolymers, show disordered motion, e.g., the Brownian motion of pollen. However, one may preferably direct bulk motion in these systems by confining them in asymmetric geometries [1–5], or applying biased external electromagnetic or chemical potentials [6–11]. Such microratchets have also shown some capability of sorting mixed species [12–15]. Here, we ask whether there is an analogous *macroratchet* that can segregate mixtures at the macroscale. Vibrofluidized grains, whose motion appears similar to that of microscopic particles, are an appropriate material to investigate in such a macroratchet.

Granular materials are ubiquitous in nature and in industry. This makes it important to study their mechanical response, which may be solidlike or fluidlike [16]. At the same time, granular mixtures often segregate when fluidized, e.g., large rocks "float" to the top in landslides [17]. This feature can be a boon or a bane depending on whether we wish to separate food grains in agroindustry, or to mix powders in a chemical process. Developing and understanding granular segregation processes is therefore also of substantial scientific and practical relevance.

*bhateja@iitb.ac.in
†ishans@iitk.ac.in
‡jayantks@iitk.ac.in

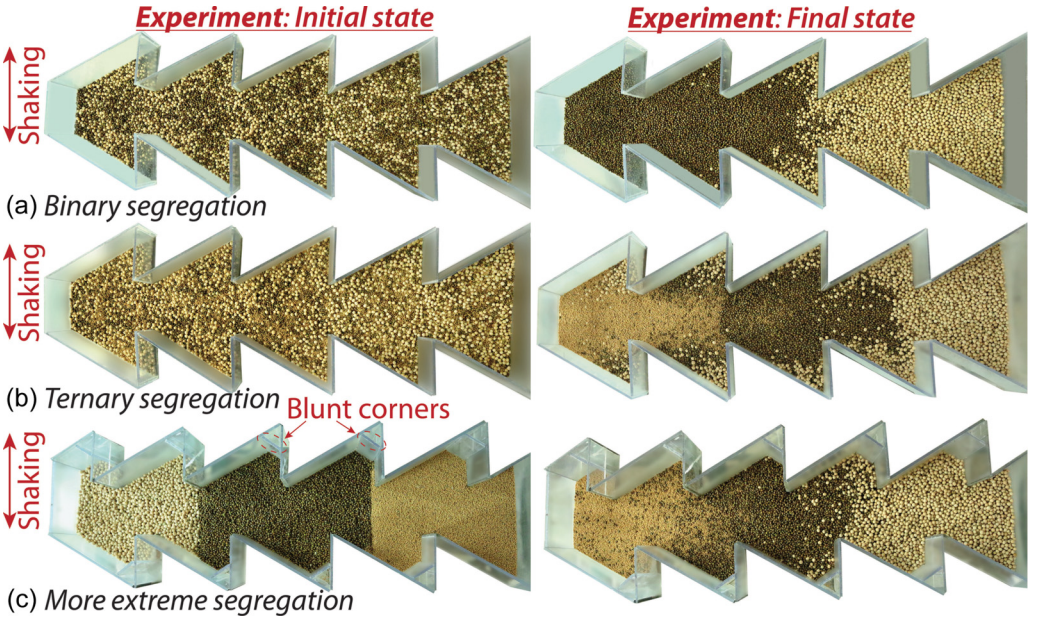

FIG. 1. *Segregation in a macroratchet.* Three experiments showing segregation in a laterally shaken, horizontal, multitrapezium channel. The left and right columns show the initial and final states. (a) A binary mixture of off-white peas (big, 7 mm diameter) and green gram (small, elongated, 3.5 mm × 5 mm). (b) A ternary mixture of peas, green gram, and yellow mustard seeds (smallest, 2 mm diameter). (c) Same mixture as in (b), but with the initial state opposite to the final segregated state obtained in (b). The experiment in (c) employs an offset and blunted multitrapezium channel that releases dead zones observed in the middle row, thereby improving segregation quality. In each experiment, grains completely segregate axially, and multiple, repeating stripes [22] are never formed. See Fig. S16 of SM [18] for a full-size figure.

II. SEGREGATION PROCESS

Figure 1 shows typical experiments with granular mixtures in a macroscale "ratchet." The ratchet is a 1-m-long channel with closed ends, comprising five concatenated trapeziums with a minimum width of 10 cm. The orientations of the trapezoidal sections distinguish the channel's right end from its left end; the sidewalls slant right at 30°. During operations, the channel is shaken laterally in a plane normal to gravity at a fixed amplitude of 7 cm. Figure 1(a) is an experiment with binary mixtures; a movie and experimental details are available in the Supplemental Material (SM) [18]. A mixture of two types of grains is poured into the channel up to a height of about four to six grains; see Fig. 1's caption for the grain data. The channel is then shaken at a frequency (ω) between 1.5 and 2.25 Hz until a steady state is achieved within 400–1600 cycles, depending on ω. At the steady state, the two types of grains are found to have segregated, and lie at opposite ends of the channel. Changing the amplitude modifies the frequency range [19–21] over which segregation is observed, and this is further discussed in Sec. 2 of SM [18]. Figures 1(b) and 1(c) show that our macroratchet is also able to segregate ternary mixtures with increasingly complex initial conditions. Experiments confirm that the final segregated state is universal, in that grains always axially segregate irrespective of the initial preparation.

The physics of segregation in the macroratchet is fundamentally distinct from that in microratchets because of the importance of gravity, and the fact that collisions between grains are dissipative; gravity is inconsequential in microratchets, while interparticle collisions—when relevant—are typically energy preserving. Furthermore, as we explain in Secs. 3–7 of SM [18], our new segregation process is not explained by presently known mechanisms of granular segregation: percolation [23],

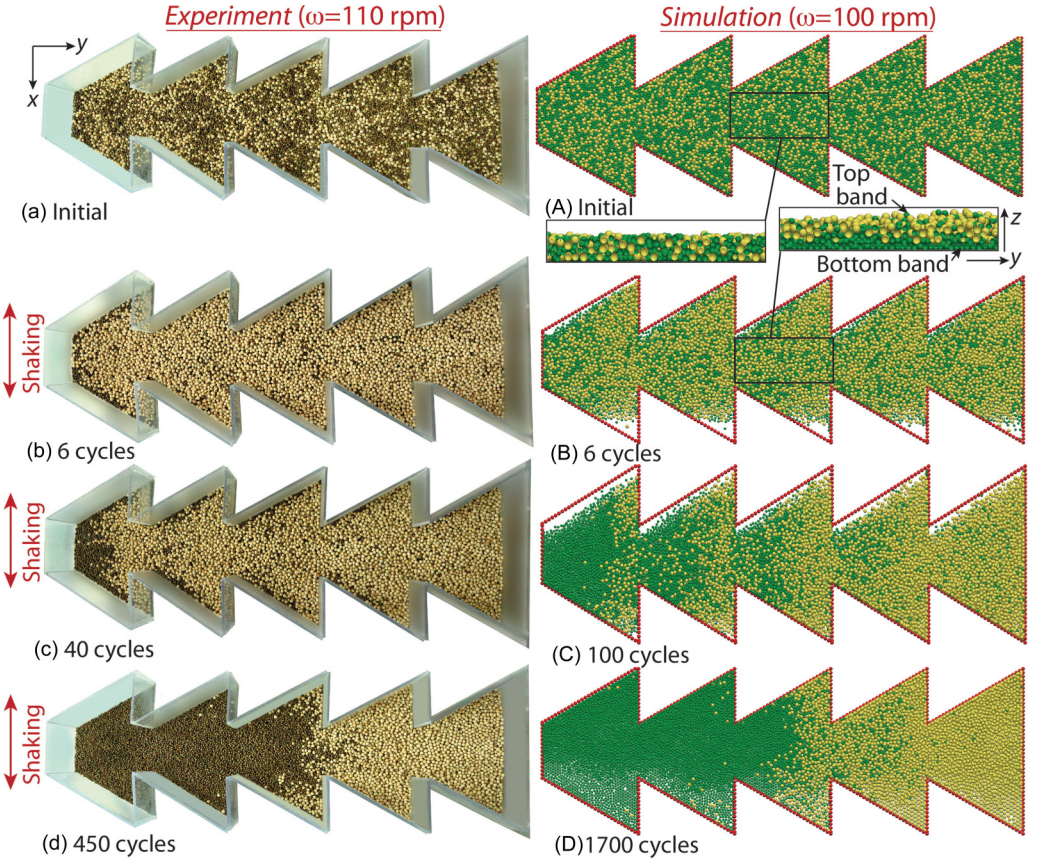

FIG. 2. *Experiment and simulation.* The left column displays stages during a typical experiment with green gram (small) and peas (big, off-white). The right column has the corresponding simulation with small (green) and big (yellow) spherical grains. Experiment: The mixture is poured into the channel in (a). Within six cycles, in (b), grains sort vertically into two horizontal bands, with big, white grains rising to the top, and small, green ones sinking to the bottom. In (c), the two bands start separating axially. Complete axial separation is observed in (d). Simulation: Simulations parallel the experimental observations. A lower frequency was employed for computational ease. The side views (in the y-z plane) of the middle section of (A) and (B) show vertical sorting.

condensation [24], convection [25–27], and differences in angles of repose [22,28], diffusion fluxes [28], and kinetic stresses [29]. These mechanisms were discovered while investigating phenomena such as the Brazil-nut effect [23,30]—wherein big grains rise to the top, its reverse [31,32], segregation in rotating drums [28,33,34], and inclined and chute flows [35–39]. Finally, we make two remarks. First, it is important to distinguish our macroratchet from seemingly analogous two-dimensional segregation [40–46] in a vertically vibrated channel with one wall patterned with many small grain-sized teeth; see Fig. S13 of SM [18]. As we detail in Sec. 8 of SM [18], the two systems differ fundamentally in construction, functioning, and physics. Second, Mobarakabadi *et al.* [47] reported the transport of a single species of dilute grains in a machine with a geometry similar to ours. In contrast, we investigate complete segregation of a dense mixture. The phenomenon described here and the physics uncovered are entirely different.

Experiments with various binary mixtures reveal the following general features, which are supported by simulations: (i) In the beginning, the mixture rapidly sorts vertically into two horizontal bands parallel to the base of the channel. This is clear from the side views of Figs. 2(A) and 2(B), and by contrasting initial states Figs. 2(a) and 2(A) with, respectively, Figs. 2(b) and 2(B); big grains are

observed to rise to the top. This vertical sorting takes far less time than the entire segregation process, as the vertical distance through which the grains move is of the order of the fill height (∼20–30 mm), which is much smaller than the channel's length. (ii) The two bands then move slowly along the axis of the channel in opposite directions, with the top band always moving to the right, as shown in Figs. 2(c) and 2(C). This axial separation stops when the grains in the top and bottom bands finish collecting at the right and left ends of the channel, respectively; see Figs. 2(d) and 2(D). (iii) Vertical and axial motions of the grains take place in widely separated dynamical regimes. This is emphasized by the fact that the average kinetic energy associated with axial separation in Fig. 2(C) is only about 3% of the total kinetic energy of the grains. (iv) Segregation occurs over a range of shaking frequencies ω (∼1.5–2.25 Hz for food grains when the amplitude is 7 cm; cf. Sec. 2 of SM [18]). Outside this frequency range, grains sort vertically, but do not separate axially. (v) All grains, when shaken alone, move rightwards. The leftward motion of the bottom band is therefore unanticipated, and is key to understanding segregation in our macroratchet.

In general, grains differ both in size and in density, and sort vertically when vibrated. This process may be familiar to us from past work [23,30–32], and is explained on the basis of either percolation [23], where small grains fall through voids between big grains, or condensation [24], in which heavier grains sink, notwithstanding their size. At the same time, when the channel is shaken laterally, repeated collisions of the grains with the slanted sides of the trapezoidal sections provide a net axial collisional flux of momentum to the grains, causing them to move right. This explains the axial motion of the top band to the right. The motion of the bottom band to the left end of the channel, opposite to the direction in which sidewalls provide axial momentum to the grains, is, however, unexpected, and needs explanation. In the remaining discussion, for clarity, we will assume that grains are of similar density but differ in size, as is true for food grains. A density difference plays a role in our experiments only when it is rather large and, even then, affects only vertical sorting; see Sec. 4 of SM [18].

III. INTERFACIAL PRESSURE-GRADIENT MECHANISM

Experiments and simulations suggest that the anomalous motion of the bottom band, towards the left end of the channel, is driven by the pressure gradient imposed upon that band by the excess piling up of the grains in the top band at the right-end wall of the channel. This pressure-gradient mechanism is explained in Fig. 3, and relies crucially upon the following: (i) the presence of a right-end wall of the channel to cause a pileup, (ii) adequate material in the top band to impose the required overburden, and (iii) the persistence of the banded structure throughout the segregation process. The latter is made possible by vertical sorting that, as already seen, occurs over much shorter time and length scales compared to axial motion; simulations (Sec. 3 of SM [18]) verify this. In this context, experiments and simulations (Sec. 6 of SM [18]) show that convection currents, observed in inclined flows [36], are not present.

We now verify the pressure-gradient mechanism of Fig. 3. Experiments (Sec. 3 of SM [18]) permit only indirect verification by producing results consistent with our hypothesis. This is because the internal visualization of dry, three-dimensional granular flows is not easy. Here, we validate the pressure-gradient mechanism through extensive parallelized [49] discrete element (DE) simulations [50,51] of binary mixtures comprising spherical grains; see Sec. 1 of SM [18] for computational details.

One such DE simulation was shown in (A)–(D) of Figs. 2 and 3. For this simulation, we compute the cross-sectionally averaged center-of-mass heights $h_b(y,t)$ and $h_s(y,t)$, and number densities $n_b(y,t)$ and $n_s(y,t)$ of the big ("b") and small ("s") grains, respectively. The extent of vertical sorting of the big and small grains will be indicated by the difference in h_b and h_s, while their axial separation is estimated by the variation of n_b and n_s along the channel's axis. Once bands form, we find the cross-sectionally averaged pressure $p(y,t)$ exerted by the grains in the top band on those in the bottom band. Figure 4 displays these quantities after nondimensionalization, along with the initial and final locations of all grains.

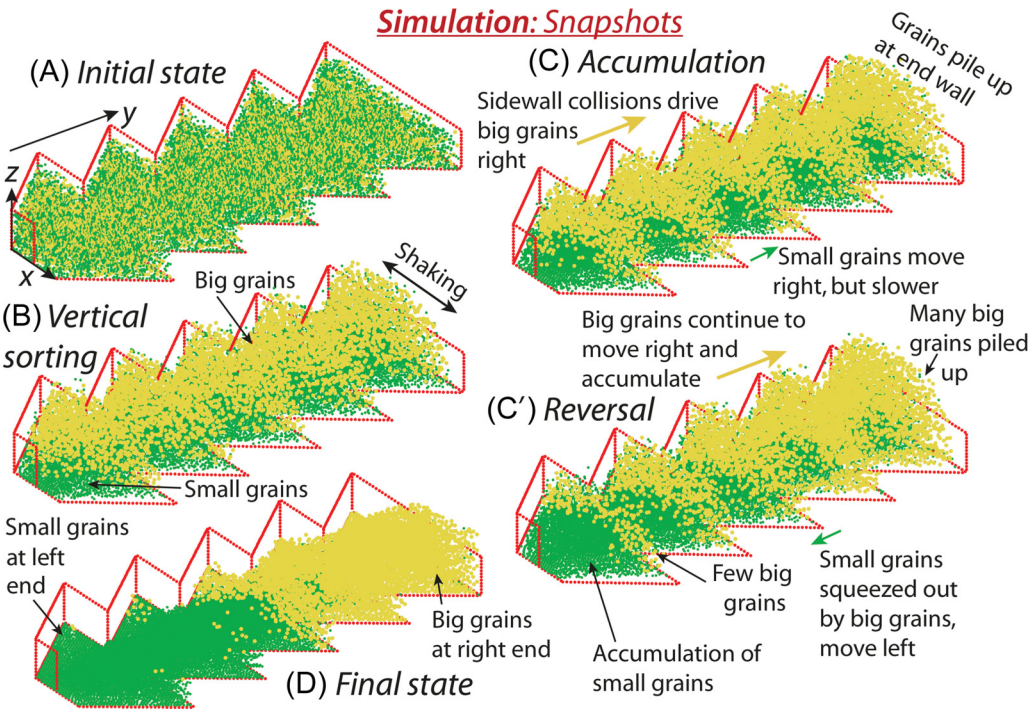

FIG. 3. *Pressure-gradient mechanism.* Three-dimensional visualization of the simulations in Figs. 2(A)–2(D). On shaking, the mixture in (A) sorts vertically into two bands in (B). In (C), repeated collisions with the slanted sidewalls push both bands towards the right end of the channel where, because of the end wall, they begin to pile up. The grains in the bottom band move slower than the grains in the top band, as they are more confined. Because of this, the top grains accumulate faster at the right-end wall. This overburden of the top grains creates a pressure gradient that squeezes the bottom band towards the channel's left end, as described in (C′). The final segregated state is shown in (D). See Fig. S17 of SM [18] for a full-size figure.

Beginning from a mixed state in Fig. 4(A), the different center-of-mass heights h_b and h_s in Fig. 4(B_1) indicates vertical separation into bands within six cycles. In this period there is no significant axial motion of grains, as confirmed by the number densities n_b and n_s not varying along the axis in Fig. 4(B_2); cf. Figs. 2(B) and 3(B). The increase to the right in the center-of-mass height and number density of both grains in, respectively, Figs. 4(C_1) and 4(C_2), shows that both bands initially move rightwards, corroborating Fig. 3(C). The greater number density of the big grains at the channel's right end in Fig. 4(C_2), in contrast to that of the small grains, verifies that the top band indeed moves faster towards the right than the bottom band.

The interface pressure p and its sectional average (solid, black line) are shown in the rightmost column of Fig. 4. This pressure displays a characteristic sawtooth pattern with sharp rises and still sharper falls within each trapezoidal section, and we discuss this aspect below. Variations in the average interface pressure closely follow the axial motion of the top band. After vertical sorting, Fig. 4(B_3) confirms that the average interface pressure is nearly uniform, in keeping with the minimal axial motion suggested by Fig. 3(B). As the bands move axially, the average interface pressure in Fig. 4(C_3) builds up gently from the channel's left end to its right end, consistent with visualization of Fig. 3(C). This global or average interfacial pressure gradient increases monotonically with time, until, under the action of the pressure imposed by the top band, the bottom band reverses its axial motion, as in Fig. 3(C′). This stage is shown in row C′ of Fig. 4, where the average interfacial pressure gradient in Fig. 4(C_3') is much steeper than in Fig. 4(C_3). Reversal of the bottom band is clear from Fig. 4(C_2') by the decrease to the right in the number density of the small grains in the

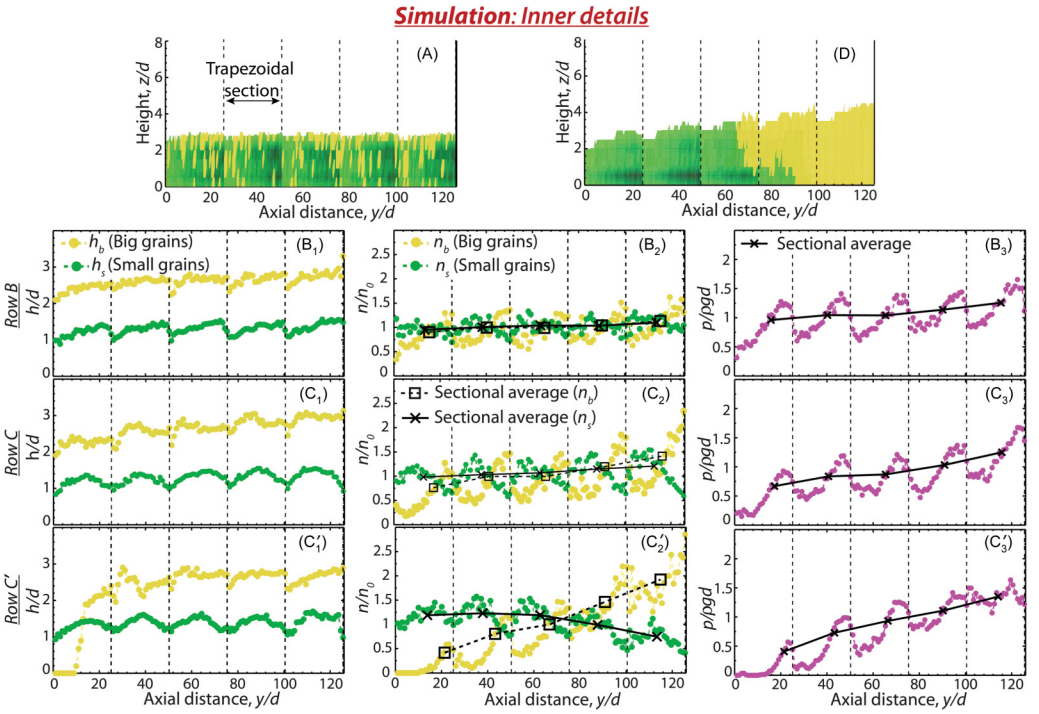

FIG. 4. *Confirming the interfacial pressure-gradient mechanism.* Top row: Side view (along x axis) of the initial (A) and final (D) states of the mixture of small (green) and big (yellow) grains simulated in Figs. 2 and 3; all grains are projected onto the y-z plane, and data are then coarse grained [48] to produce a smooth two-dimensional density map. Rows B, C, C′: Correspond to stages (B), (C), and (C′) of Fig. 3. Left, center, and right columns display, respectively, cross-sectionally averaged and scaled, center-of-mass height (h/d), number density (n/n_0), and interface pressure ($p/\rho gd$), where ρ and d are the density and diameter of the big grains, g is the gravitational acceleration, and n_0 is the number density of grains when spread uniformly in the channel.

bottom band; cf. Fig. 4(C_2). At this time, Fig. 4(C_1') indicates an absence of big grains at the left end of the channel. The bottom band continues to move leftwards until the steady segregated state seen in (D) of Figs. 2–4 is achieved. At its greatest, in Fig. 4(C_3'), the scaled average interfacial pressure gradient $d(p/\rho gd)/d(y/d)$ was a mere 0.0092, corresponding to a change in height of about two big grain diameters ($d = 7$ mm) over the meter-long channel. Employing $\rho \approx 1200\ \mathrm{kg/m^3}$, we compute the actual average interfacial pressure gradient to be about 100 Pa/m, not very much larger than the few Pa/m pressure gradients involved in the flow of ice sheets [52].

The average interfacial pressure gradient depends on the presence of the right-end wall that causes the grains in the top band to pile up. On the other hand, variations in interface pressure within a trapezoidal section are caused by lateral constrictions, normal to the channel's axis, where two sections join, as shown in Fig. 1. However, it is the gentle average interfacial pressure gradient which is critical to segregation. We prove this by repeating the simulations of Fig. 2 in a channel with infinitely many trapezoidal sections. Such an "infinite" ratchet has no end walls, and is created by imposing periodic boundary conditions at its left and right ends (particles exiting right reenter from the left, and vice versa). We find from Fig. 5(a) that grains still sort vertically into two horizontal bands, and then, gathering axial momentum from collisions with the slanted sidewalls, move together from the channel's left to its right, as is clear from axial velocities plotted in Fig. 5(b). No axial separation is seen. As in a closed channel, interface pressure still varies within a section, but, in

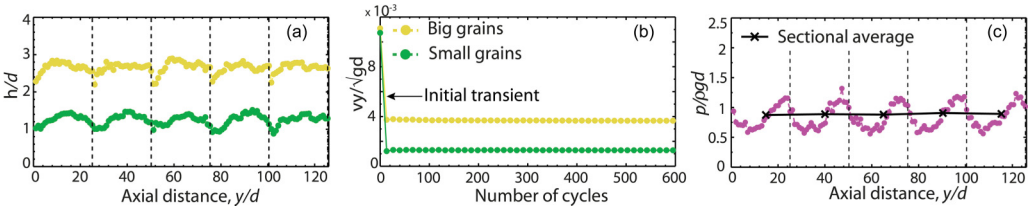

FIG. 5. *Average interfacial pressure-gradient:* Simulation of the mixture of Fig. 2(A) in a multitrapezium channel with periodic boundary conditions replacing end walls. Steady-state (a) center-of-mass heights and (b) average velocities ($v_y/\sqrt{gd}$) of both grains, and (c) interface pressure are shown.

contrast, no average interfacial pressure gradient is developed; see Fig. 5(c). Similarly, experiments done in an open channel (no end walls) show no segregation, and all grains exit from the right end.

The interfacial pressure-gradient mechanism also elucidates ternary segregation of Figs. 1(b) and 1(c) as follows: On shaking, the mixture sorts vertically into three bands, with the smallest and biggest grains constituting the bottom and top bands, respectively. Sidewall collisions drive these bands rightwards, with the top band moving the fastest and the bottom band, which is most confined, being the slowest. Grains pile up at the right-end wall, creating interfacial pressure gradients that cause lower bands to get squeezed leftwards by the band above. Thus, grains segregate in an increasing order of size from the channel's left end to its right end.

IV. CONCLUSIONS

We report a macroscale analog of microratcheting systems, which segregates multicomponent granular mixtures. This will have important consequences in furthering our understanding of granular segregation processes, which are frequently observed in nature and in industry. The underlying physics of the macroratchet is very different from the one governing microratchets. At the same time, segregation in the macroratchet was not explained by the classical theories of granular segregation considered here. This led to the discovery of a new segregation mechanism in granular materials, which relied on dynamics in three orthogonal directions over two very different time scales: Laterally shaken grains first rapidly sort vertically into horizontal granular bands that are then axially separated by strikingly gentle average interfacial pressure gradients acting over long distances. The computational detection of this interfacial pressure-gradient mechanism was nontrivial, as it required estimating small spatial and temporal variations in the average interface pressures between two dynamically interacting, rapidly agitated granular species. Remarkably, even while the motion of grains in our macroratchet resembles randomly agitated particles in microscopic ratchets, its averaged underlying physics is closer to that observed in much larger-scale geophysical fluid dynamical processes. Indeed, the slow axial separation of horizontal granular bands over long distances under the action of gentle average interfacial pressure gradients prompts comparison with gravity currents [53,54], and hints at an unexplored connection between fluid flow and granular flow and segregation.

ACKNOWLEDGMENTS

We acknowledge financial support of Department of Science and Technology (DST) Grant No. SR/S3/CE/0053/2010, Government of India. We thank members of the Mechanics & Applied Mathematics Group, especially Anindya Chatterjee and Sivasambu Mahesh, and also Ashish Orpe (NCL, Pune) for helpful discussions. We also thank Satya Prakash Mishra for help with experiments, and Vipin Sharma, Sunit Gupta, and Koumudi Patil (Yukti Lab, IIT Kanpur) for help with the movie and figures.

[1] H. Linke, T. E. Humphrey, A. Lofgren, A. O. Sushkov, R. Newbury, R. P. Taylor, and P. Omling, Experimental tunneling ratchets, Science **286**, 2314 (1999).
[2] A. van Oudenaarden and S. G. Boxer, Brownian ratchets: Molecular separations in lipid bilayers supported on patterned arrays, Science **285**, 1046 (1999).
[3] J. S. Bader, R. W. Hammond, S. A. Henck, M. W. Deem, G. A. McDermott, J. M. Bustillo, J. W. Simpson, G. T. Mulhern, and J. M. Rothberg, DNA transport by a micromachined brownian ratchet device, Proc. Natl. Acad. Sci. USA **96**, 13165 (1999).
[4] J. E. Villegas, S. Savelëv, F. Nori, E. M. Gonzalez, J. V. Anguita, R. Garcia, and J. L. Vicent, A superconducting reversible rectifier that controls the motion of magnetic flux quanta, Science **302**, 1188 (2003).
[5] S. Matthias and F. Muller, Asymmetric pores in a silicon membrane acting as massively parallel Brownian ratchets, Nature (London) **424**, 53 (2003).
[6] C. S. Lee, B. Janko, I. Derenyi, and A. L. Barabasi, Reducing vortex density in superconductors using the "ratchet effect," Nature (London) **400**, 337 (1999).
[7] J. Rousselet, L. Salome, A. Ajdari, and J. Prost, Directional motion of Brownian particles induced by a periodic asymmetric potential, Nature (London) **370**, 446 (1994).
[8] A. Engel, H. W. Muller, P. Reimann, and A. Jung, Ferrofluids as Thermal Ratchets, Phys. Rev. Lett. **91**, 060602 (2003).
[9] S. Ghosh, A. K. Sood, and N. Kumar, Carbon nanotube flow sensors, Science **299**, 1042 (2003).
[10] T. Salger, S. Kling, T. Hecking, C. Geckeler, L. Morales-Molina, and M. Weitz, Directed transport of atoms in a Hamiltonian quantum ratchet, Science **326**, 1241 (2009).
[11] M. V. Costache and S. O. Valenzuela, Experimental spin ratchet, Science **330**, 1645 (2010).
[12] L. R. Huang, E. C. Cox, R. H. Austin, and J. C. Sturm, Continuous particle separation through deterministic lateral displacement, Science **304**, 987 (2004).
[13] G. Mahmud, C. J. Campbell, K. J. M. Bishop, Y. A. Komarova, O. Chaga, S. Soh, S. Huda, K. Kandere-Grzybowska, and B. A. Grzybowski, Directing cell motions on micropatterned ratchets, Nat. Phys. **5**, 606 (2009).
[14] L. Gao, M. A. Tahir, L. N. Virgin, and B. B. Yellen, Multiplexing superparamagnetic beads driven by multi-frequency ratchets, Lab Chip **11**, 4214 (2011).
[15] L. Bogunovic, R. Eichhorn, J. Regtmeier, D. Anselmetti, and P. Reimann, Particle sorting by a structured microfluidic ratchet device with tunable selectivity: Theory and experiment, Soft Matter **8**, 3900 (2012).
[16] H. M. Jaeger and S. R. Nagel, Physics of the granular state, Science **255**, 1523 (1992).
[17] C. G. Johnson, B. P. Kokelaar, R. M. Iverson, M. Logan, R. G. LaHusen, and J. M. N. T. Gray, Grain-size segregation and levee formation in geophysical mass flows, J. Geophys. Res. **117**, F01032 (2012).
[18] See Supplemental Material at http://link.aps.org/supplemental/10.1103/PhysRevFluids.2.052301 for a video of binary segregation in the granular ratchet, and a text file containing supporting information.
[19] C. R. Wassgren, C. E. Brennen, and M. L. Hunt, Vertical vibration of a deep bed of granular material in a container, J. Appl. Mech. **63**, 712 (1996).
[20] P. Eshuis, K. Van Der Weele, D. Van Der Meer, R. Bos, and D. Lohse, Phase diagram of vertically shaken granular matter, Phys. Fluids **19**, 123301 (2007).
[21] A. Bhateja, I. Sharma, and J. K. Singh, Scaling of granular temperature in vibro-fluidized grains, Phys. Fluids **28**, 043301 (2016).
[22] O. Zik, D. Levine, S. G. Lipson, S. Shtrikman, and J. Stavans, Rotationally Induced Segregation of Granular Materials, Phys. Rev. Lett. **73**, 644 (1994).
[23] A. Rosato, K. J. Strandburg, F. Prinz, and R. H. Swendsen, Why the Brazil Nuts are on Top: Size Segregation of Particulate Matter by Shaking, Phys. Rev. Lett. **58**, 1038 (1987).
[24] D. C. Hong, P. V. Quinn, and S. Luding, Reverse Brazil-Nut Problem: Competition between Percolation and Condensation, Phys. Rev. Lett. **86**, 3423 (2001).
[25] J. B. Knight, H. M. Jaeger, and S. R. Nagel, Vibration Induced Size Separation in Granular Media: The Convection Connection, Phys. Rev. Lett. **70**, 3728 (1993).
[26] M. Medved, D. Dawson, H. M. Jaeger, and S. R. Nagel, Convection in horizontally vibrated granular material, Chaos **9**, 691 (1999).

[27] E. L. Grossman, Effects of container geometry on granular convection, Phys. Rev. E **56**, 3290 (1997).
[28] J. M. Ottino and D. V. Khakhar, Mixing and segregation of granular materials, Annu. Rev. Fluid Mech. **32**, 55 (2000).
[29] Y. Fan and K. M. Hill, Theory for shear-induced segregation of dense granular mixtures, New J. Phys. **13**, 095009 (2011).
[30] M. E. Möbius, B. E. Lauderdale, S. R. Nagel, and H. M. Jaeger, Brazil-nut effect: Size separation of granular particles, Nature (London) **414**, 270 (2001).
[31] T. Shinbrot and F. J. Muzzio, Reverse Buoyancy in Shaken Granular Beds, Phys. Rev. Lett. **81**, 4365 (1998).
[32] T. Shinbrot, Granular materials: The Brazil nut effect—in reverse, Nature (London) **429**, 352 (2004).
[33] C. R. K. Windows-Yule, B. J. Scheper, A. J. van der Horn, N. Hainsworth, J. Saunders, D. J. Parker, and A. R. Thornton, Understanding and exploiting competing segregation mechanisms in horizontally rotated granular media, New J. Phys. **18**, 023013 (2016).
[34] P. Richard and N. Taberlet, Recent advances in DEM simulations of grains in a rotating drum, Soft Matter **4**, 1345 (2008).
[35] S. B. Savage and C. K. K. Lun, Particle size segregation in inclined chute flow of dry cohesionless granular solids, J. Fluid Mech. **189**, 311 (1988).
[36] J. M. N. T. Gray and V. A. Chugunov, Particle-size segregation and diffusive remixing in shallow granular avalanches, J. Fluid Mech. **569**, 365 (2006).
[37] S. Wiederseiner, N. Andreini, G. Épely Chauvin, G. Moser, M. Monnereau, J. M. N. T. Gray, and C. Ancey, Experimental investigation into segregating granular flows down chutes, Phys. Fluids **23**, 013301 (2011).
[38] Y. Fan and K. M. Hill, Phase Transitions in Shear-Induced Segregation of Granular Materials, Phys. Rev. Lett. **106**, 218301 (2011).
[39] D. V. Khakhar, J. J. McCarthy, and J. M. Ottino, Mixing and segregation of granular materials in chute flows, Chaos **9**, 594 (1999).
[40] Z. Farkas, P. Tegzes, A. Vukics, and T. Vicsek, Transitions in the horizontal transport of vertically vibrated granular layers, Phys. Rev. E **60**, 7022 (1999).
[41] D. C. Rapaport, The wonderful world of granular ratchets, Comput. Phys. Commun. **147**, 141 (2002).
[42] D. C. Rapaport, Mechanism for granular segregation, Phys. Rev. E **64**, 061304 (2001).
[43] M. Levanon and D. C. Rapaport, Stratified horizontal flow in vertically vibrated granular layers, Phys. Rev. E **64**, 011304 (2001).
[44] Z. Farkas, F. Szalai, D. E. Wolf, and T. Vicsek, Segregation of granular binary mixtures by a ratchet mechanism, Phys. Rev. E **65**, 022301 (2002).
[45] J. F. Wambaugh, C. Reichhardt, and C. J. Olson, Ratchet-induced segregation and transport of nonspherical grains, Phys. Rev. E **65**, 031308 (2002).
[46] X. Shi, G. Miao, and H. Zhang, Horizontal segregation in a vertically vibrated binary granular system, Phys. Rev. E **80**, 061306 (2009).
[47] S. Mobarakabadi, E. N. Oskoee, M. Schröter, and M. Habibi, Granular transport in a horizontally vibrated sawtooth channel, Phys. Rev. E **88**, 042201 (2013).
[48] T. Weinhart, A. R. Thornton, S. Luding, and O. Bokhove, From discrete particles to continuum fields near a boundary, Granular Matter **14**, 289 (2012).
[49] M. J. Quinn, *Parallel Programming in C with MPI and OpenMP* (McGraw-Hill, New York, 2003).
[50] P. A. Cundall and O. D. L. Strack, A discrete numerical model for granular assemblies, Geotechnique **29**, 47 (1979).
[51] D. Zhang and W. J. Whiten, The calculation of contact forces between particles using spring and damping models, Powder Technol. **88**, 59 (1996).
[52] H. A. Fricker and L. Padman, Ice shelf grounding zone structure from ICESat laser altimetry, Geophys. Res. Lett. **33**, L15502 (2006).
[53] J. E. Simpson, Gravity currents in the laboratory, atmosphere, and ocean, Annu. Rev. Fluid Mech. **14**, 213 (1982).
[54] R. A. V. Robison, H. E. Huppert, and M. G. Worster, Dynamics of viscous grounding lines, J. Fluid Mech. **648**, 363 (2010).